Cancer Chemother Pharmacol (1998) 42: 9–16

ORIGINAL ARTICLE

Yoshihiro Masuda · Hiroyuki Kobayashi
James F. Holland · Takao Ohnuma

Reversal of multidrug resistance by a liposome-*MDR*1 ribozyme complex

Received: 18 June 1997 / Accepted: 8 October 1997

Abstract *Purpose*: Multidrug resistance (MDR) is a major obstacle in cancer chemotherapy. We examined whether cationic liposome-mediated transfer of a ribozyme could reverse MDR. *Methods*: A ribozyme which cleaved codon 196 of *MDR*1 mRNA was constructed from synthetic oligonucleotides. The *MDR*1 ribozyme was mixed with *N*-(1-(2,3-dileoyloxy)propyl)-*N*,*N*,*N*-trimethylammonium methyl sulfate (DOTAP) to form a liposomal complex. The complex was used to treat two P-glycoprotein-producing MDR cell lines: MCF-7/R human breast cancer cells resistant to doxorubicin and MOLT-3/TMQ_{800} human ALL cells resistant to trimetrexate (TMQ). In order to investigate the differential sensitivity of these two cell lines to the liposome-ribozyme complex, cellular pharmacological studies including phase-contrast and confocal microscopic studies were performed. *Results*: Treatment with the liposome-ribozyme complex resulted in reversal of vincristine (VCR) resistance in MCF-7/R cells, but not in MOLT-3/TMQ_{800} cells. In MCF-7/R cells the treatment resulted in decreases in *MDR*1 mRNA expression and P-glycoprotein production, whereas no changes in these parameters were seen in MOLT-3/TMQ_{800} cells. Phase-contrast microscopy revealed that in MCF-7/R cells treatment with DOTAP led to the formation of cytoplasmic vacuoles, and treatment with latex beads resulted in the development of a shiny material in the cytoplasm. In contrast, in MOLT-3/TMQ_{800} cells hardly any morphological changes occurred. Confocal microscopic imaging showed cytoplasmic fluorescence in MCF-7/R cells after treatment with DOTAP/FITC-dextran or FITC-conjugated latex beads. In MOLT-3/TMQ_{800} cells no fluorescence was detected. Treatment with cytochalasin B abolished fluorescence in MCF-7/R cells after treatment with DOTAP/FITC-dextran or FITC-conjugated latex beads. These studies show that MCF-7/R cells have high endocytotic activity whereas MOLT-3/TMQ_{800} cells have little activity. *Conclusions*: Endocytotic activity was correlated with the success of cationic liposome-mediated transfer of *MDR*1 ribozyme. Determination of endocytotic activity of target tumor cells may be predictive of efficacy of liposome-mediated gene transfer.

Key words Multidrug resistance · *MDR*1 · Cationic liposome · Ribozyme · Endocytosis

Abbreviations *MDR* multidrug resistance · *DXR* doxorubicin · *TMQ* trimetrexate · *FBS* fetal bovine serum · *DOTAP* N-(1-(2,3-dileoyloxy)propyl)-*N*,*N*,*N*-trimethylammonium methyl sulfate · *VCR* vincristine · *MTT* 3-(4,5-dimethylthiazol-2-yl)-2,5-diphenyltetrazolium bromide · *PBS* Dulbecco's phosphate-buffered saline · *FITC* fluorescein isothiocyanate

Y. Masuda · J.F. Holland · T. Ohnuma
Division of Neoplastic Diseases,
Samuel Bronfman Department of Medicine,
Mount Sinai School of Medicine,
New York, NY 10029, USA

H. Kobayashi
Department of Laboratory Medicine,
National Defense Medical College,
Tokorozawa, Saitama 359, Japan

T. Ohnuma (✉)
Division of Neoplastic Diseases, Box 1128,
Mount Sinai Medical Center,
One Gustave L. Levy Place, New York, NY 10029-6574, USA
Tel.: 212-241-6664; Fax: 212-423-9458;
E-mail: ohnuma@msvax.mssm.edu

Introduction

MDR is a universal phenomenon in cancer chemotherapy in humans. One major mechanism for this phenomenon is the overexpression of the *MDR*1 gene, a product of which is P-glycoprotein. P-glycoprotein, a 170-kDa transmembrane protein, acts as an energy-dependent drug efflux pump [1–4] and keeps intracellular drug concentrations low. Since amplification of the

*MDR*1 gene is not a prerequisite to P-glycoprotein-related resistance in human tumor cells [5–7], *MDR*1 mRNA or P-glycoprotein itself can be a potential target of inhibition. One means to inhibit the translation of *MDR*1 mRNA to P-glycoprotein is to use a ribozyme or a catalytic RNA targeted to *MDR*1 mRNA [8, 9].

There are two ways to deliver the ribozyme to the target mRNA [10]. One way is by endogenous delivery. This is the intracellular transcription of a ribozyme coding gene and is accomplished by the transfection or infection of ribozyme-producing vectors into target cells. We and others have shown that this approach is effective in reversing the MDR phenotype [11, 12]. The other way is by exogenous delivery, in which the ribozymes are introduced into the cells either directly by injection, simply by addition to the cells in culture, or by transfection. In recent years, the latter strategy has been used with the aid of cationic liposome-mediated transfer. We examined cationic liposome-mediated delivery of *MDR*1 ribozyme in two MDR cell lines.

Materials and methods

Cell lines

The parent MCF-7 human breast carcinoma cell line and a MDR subline MCF-7/R (190-fold resistant to DXR) [13] were obtained from Dr. Steven D. Averbuch and maintained in DMEM medium (BioWhittaker, Walkersville, Md.) containing 10% FBS (Sigma, St. Louis, Mo.) and 3×10^{-3} units/ml human insulin (Novo Nordisk Pharmaceuticals, Princeton, N.J.) at 37 °C in a humidified atmosphere containing 5% CO_2. The parent MOLT-3 human acute lymphoblastic leukemia cell line [14] and the MDR subline MOLT-3/TMQ_{800} (800-fold resistant to TMQ) [11] were maintained in RPMI-1640 medium (BioWhittaker) containing 10% FBS.

Ribozyme synthesis

*MDR*1 ribozyme targeted to the GUC sequence in the 196 amino acid codon was synthesized as described previously [11]. Initially, two deoxyoligonucleotides were made by Genset (La Jolla, Calif.): the top strand contained the T7 RNA polymerase promoter region (5′-ATTAATACGACTCACTATAGGG-3′) and the bottom strand both the T7 RNA polymerase promoter region and the template sequence (5′-TCTTTCAGTTTCGTCCTCACGGACT CATCAGAATGGCAACCCCTATAGTGAGTCGTATTAAT-3′). Templates were prepared by heating the two DNA strands together to 80°C for 2 min and then slowly cooling to room temperature. The transcription of RNA from the annealed synthetic DNA templates was carried out as described by Milligan et al. [15].

Liposome-mediated ribozyme transfection and cytotoxic assay

As a preliminary study, we examined the cytotoxic effect of the cationic liposome, DOTAP, (Fig. 1; Boehringer Mannheim, Indianapolis, Ind.) alone. On day 0, the cells described above in an exponential growth phase were washed with PBS without Ca^{2+} and Mg^{2+} (BioWhittaker) and resuspended in a reduced serum medium (Opti-MEM I, GIBCO-BRL, Grand Island, N.Y.). Reduced serum medium was used on the first day of transfection to overcome the effects of inhibitory components [16]. The final concentrations of DOTAP ranged from 0.01 to 1.0 μg/200 μl per well in a 96-well flat-bottom plate (Becton Dickinson, Lincoln Park, N.J.). Half of the medium was exchanged with fresh medium containing DOTAP every day. After 5 days of incubation at 37 °C, cytotoxic effects were measured by an MTT assay using a Microplate Reader (Genetic Systems, Redmond, Wash.) at a wavelength of 540 nm [11].

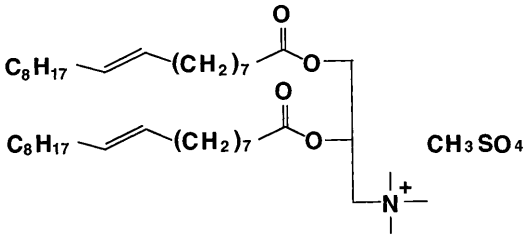

Fig. 1 Chemical structure of DOTAP.

Next, we examined the cytotoxic activity of a complex formed from DOTAP and *MDR*1 ribozyme. The complex was formed by mixing DOTAP and the ribozyme at various concentrations in 20 m*M* Hepes buffer in a final volume of 1 ml followed by incubation at room temperature for 15 min. The complex was made every day just before use. Then 100 μg/ml of recombinant RNase inhibitor (rRNasin, Promega, Madison, Wis.) was added to the complex solution. The final concentrations of DOTAP was 0.7 μg and of the ribozyme were 0.07–7.0 μg per 200 μl per well. After 5 days of incubation, cytotoxic effects were measured by the MTT assay.

Subsequent to these optimization studies, we examined whether the liposome-ribozyme complex was able to reverse MDR. Cells were cultured in the presence of the complex as described above. The exchanges of medium and the complex were performed in the same manner and schedule as described above. With the exchange of medium and the complex, one-tenth volume of various concentrations of VCR was added every 24 h on days 2–4. On day 5, the cytotoxic activity of VCR was examined by the MTT assay.

Expression of *MDR*1 gene

The expression of the *MDR*1 gene was investigated by Northern and Western blot analyses. For this purpose, 1-ml aliquots of cell suspension containing 1×10^4 cells per well were placed in a 24-well plate (Becton Dickinson) and 10 μl liposome-ribozyme complex was added to each well with final concentrations of 3.5 μg/ml DOTAP and the 17.5 μg/ml ribozyme. Changes of medium and addition of the liposome-ribozyme complex were done daily following the schedule described above. VCR was not added. Northern and Western blot analyses were performed using a standard protocol (see legend to Fig. 4).

Phase-contrast microscopy

The endocytotic activity of MCF-7/R and MOLT-3/TMQ_{800} cells was evaluated by phase-contrast microscopy. For MCF-7/R cells, 3×10^3 cells were seeded in 200 μl of reduced serum medium per well of eight-well chamber slides (Nunc, Naperville, Ill.). Three groups of samples were prepared. The first group was not treated and after 24 h incubation one-half of the medium was replaced with fresh medium containing 20% serum only. The second group was incubated with 0.7 μg DOTAP. After 24 h incubation, one-half of the medium was replaced with fresh medium containing 20% serum and 0.35 μg of DOTAP. The third group was incubated with 2 μl of a suspension of latex beads (10% v/v) with a diameter of 0.24 μm (Sigma). After 24 h incubation one-half of the medium was replaced with fresh medium containing 20% serum and 1 μl of a suspension of latex beads. Cells of all three groups were then incubated for another 24 h. After a total of 48 h incubation, cells were washed and examined immediately with a phase-contrast microscope (Olympus BX-60, Olympus, Tokyo, Japan).

For MOLT-3/TMQ_{800} cells, 3×10^4 cells were seeded in 2 ml of reduced serum medium in culture tubes. Three groups of samples

were prepared as described above. After 48 h incubation, cells were washed and attached to glass slides using a Cytospin 2 (Shandon, Pittsburgh, Pa.) for microscopic observation.

Confocal microscopy

Aliquots of 3×10^3 MCF-7/R cells were seeded in 200 µl of reduced serum medium per well of the eight-well chamber slides. Four groups of samples were prepared. The first group was not treated. The second group was incubated with 3.5 µg FITC-dextran (MW 10 000 Da, Sigma) per well. The third group was incubated with 3.5 µg FITC-dextran and 0.7 µg DOTAP per well. Before adding to the cell culture, FITC-dextran and DOTAP were mixed and incubated at room temperature for 15 min in a total volume of 10 µl in order to form a DOTAP-FITC-dextran complex. After a 24-h incubation, one-half of the medium was replaced with fresh medium containing 20% serum only or together with FITC-dextran or premixed FITC-dextran and DOTAP for the respective three groups. Cells of all three groups were then incubated for another 24 h. The fourth group was incubated with 8 µl of a suspension of FITC-conjugated latex beads (2.55% v/v) with a diameter of 0.213 µm (Fluoresbrite YG microspheres, Polysciences, Warrington, Pa.). After 48 h (first three groups) or 24 h (fourth group) incubation, cells were washed, fixed with methanol at −20 °C for 15 min and subjected to confocal imaging.

In order to confirm whether the DOTAP uptake by MCF-7/R cells was a result of endocytosis, four additional cell samples were prepared. The two samples were pretreated with 10 µg/ml cytochalasin B (Sigma) for 30 min at 37 °C. After the pretreatment, the cell samples were washed with PBS and further incubated with DOTAP-FITC-dextran complex for 24 h or FITC-conjugated latex beads for 30 min at 37 °C in the continued presence of cytochalasin B. After the incubation, cells were washed and fixed as described above. The other two samples were run simultaneously using PBS instead of cytochalasin B.

For MOLT-3/TMQ_{800} cells, 3×10^4 cells in exponential growth phase were seeded in 2 ml of reduced serum medium in culture tubes. Four groups were prepared and treated using the same schedule and concentration of FITC-dextran, DOTAP-FITC-dextran complex and FITC-conjugated latex beads as described above. After incubation, the cells were washed, attached to glass slides using a Cytospin 2, and fixed as described above.

Results

The results of the study of the cytotoxic effect of liposomes alone are shown in Table 1. More than 90% of both MCF-7/R and MOLT-3/TMQ_{800} cells were alive in the presence of 0.7 µg/200 µl or less of DOTAP. Therefore, all subsequent experiments were carried out at a DOTAP concentration of 0.7 µg/200 µl. The results of the study of the cytotoxic effects of the liposome-ribozyme complexes are shown in Table 2. The complexes formed with the ribozymes at the concentrations studied were not more toxic than DOTAP alone. Under

Table 1 Cytotoxic effects of DOTAP. On day 0, 3×10^3 cells/200 µl Opti-MEM I per well were seeded into 96-well flat-bottom plates in triplicate. Then, 10-µl aliquots of various concentrations of DOTAP diluted in 20 m*M* Hepes buffer were added to the wells. After 24 h incubation at 37 °C (day 1), one-half of the medium by volume (100 µl) was carefully aspirated so as not to disturb the cells in the bottom of the wells and exchanged with an equal volume of fresh DMEM or RPMI-1640 medium containing 20% FBS and the same concentration of DOTAP as on day 0. The cells were then incubated for another 96-h. During the 96 h incubation period, one-half of the medium by volume (100 µl) was replaced by 100 µl of fresh medium containing 10% FBS and the same concentration of DOTAP as on day 0 every 24 h. Cytotoxicity is shown as viable cell numbers (percent of control) after incubation with DOTAP. Each result is the mean of two independent experiments carried out in triplicate. All experimental values were within 10% of the mean

	DOTAP (µg/200 µl)						
	0	0.01	0.1	0.3	0.5	0.7	1.0
MCF-7/R	100	101	102	98	94	90	59
MOLT-3/TMQ_{800}	100	103	101	100	98	90	50

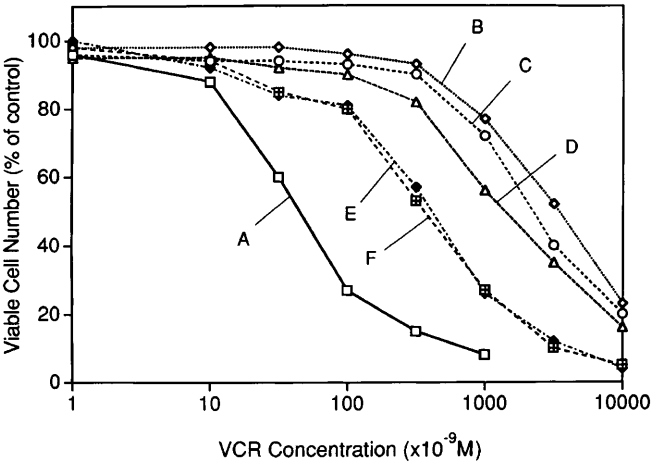

Fig. 2 Reversal of drug resistance in MCF-7/R cells (*line A* MCF-7 cells, *line B* MCF-7/R cells, *line C* MCF-7/R cells treated with DOTAP-*MDR*1 ribozyme complex for 5 days at a ribozyme concentration of 0.7 µg/200 µ1, *lines D, E and F* identical treatment at ribozyme concentrations of 1.4, 3.5 and 7.0 µg/200 µl, respectively). Each data point is the mean of two independent experiments carried out in triplicate. All experimental values were within 15% of the mean

Table 2 Cytotoxic effect of the DOTAP-*MDR*1 ribozyme complex. The complex was formed from DOTAP and the ribozyme at the concentrations shown. On day 0, 3×10^3 cells/200 µl Opti-MEM I were seeded per well into the 96-well flat-bottom plates in triplicate. Then, 10-µl aliquots of DOTAP-ribozyme complex were added to each well and incubated at 37 °C for 5 days. The medium exchange was performed every 24 h for 4 consecutive days in the same manner as described in Table 1. With the medium change, one-half of the DOTAP-ribozyme complex was also exchanged to maintain the concentrations. Control wells received 20 m*M* Hepes buffer only. Cytotoxicity is shown as viable cell numbers (percent of control) after incubation with the complex. Each value is the mean of two independent experiments carried out in triplicate. All experimental values were within 10% of the mean

	DOTAP/*MDR*1 ribozyme (µg/200 µl)									
	0/0	0.7/0	0.7/0.07	0.7/0.14	0.7/0.35	0.7/0.7	0.7/1.4	0.7/3.5	0.7/7.0	1.0/5.0
MCF-7/R	100	90	92	94	92	94	95	94	95	72
MOLT-3/TMQ_{800}	100	90	91	94	96	98	95	95	96	64

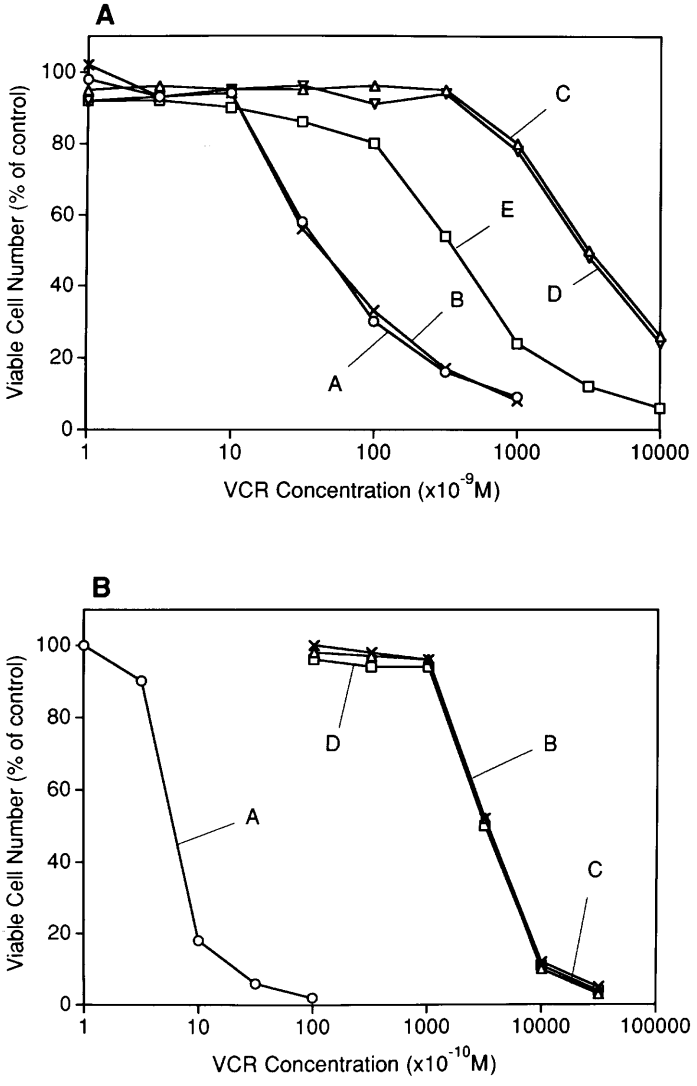

Fig. 3 A Dose-effect curves of MCF-7 and MCF-7/R cells (*line A* untreated MCF-7 cells, *line B* MCF-7 cells treated with DOTAP (0.7 μg/200 μl) alone for 5 days, *line C* untreated MCF-7/R, *line D* MCF-7/R cells treated with DOTAP alone for 5 days, *line E* MCF-7/R cells treated with DOTAP-*MDR*1 ribozyme complex for 5 days). The dose-effect curves of MCR-7 cells treated with DOTAP alone for 1 day only, with *MDR*1 ribozyme only for 5 days, or with DOTAP-*MDR*1 ribozyme complex for 1 day only or for 5 days, all overlapped with lines A and B. The dose-effect curves of MCF-7/R cells treated with DOTAP alone for 1 day only, with *MDR*1 ribozyme only for 5 days, or with DOTAP-ribozyme complex for 1 day all overlapped with lines C and D. These curves were omitted from the graph for clarity. Concentrations of DOTAP and the *MDR*1 ribozyme were 0.7 μg/200 μl and 3.5 μg/200 μl, respectively. **B** Dose-effect curves of MOLT-3 and MOLT-3/TMQ_{800} cells (*line A* MOLT-3 cells treated with DOTAP alone for 5 days, which was identical to that of untreated MOLT-3 cells, *line B* untreated MOLT-3/TMQ_{800} cells, *line C* MOLT-3/TMQ_{800} cells treated with DOTAP alone for 5 days, *line D* MOLT-3/TMQ_{800} cells treated with the complex for 5 days). All the other treatments described for MCF-7 and MCF-7/R were tested in MOLT-3 and MOLT-3/TMQ_{800} cells and the dose-effect curves were found to overlap with those for untreated cells. Each data point is the mean of two independent experiments carried out in triplicate. All experiments values were within 15% of the mean

these conditions the complexes also had no effect on the attachment of MCF-7/R cells to the bottom of the wells (data not shown). This allowed us to add the complex on day 0.

The degree of reversal of MDR in MCF-7/R cells by liposome-mediated transfer of various amounts of ribozyme is shown in Fig. 2. The maximal reversing activity was observed at 3.5 μg/200 μl of the ribozyme. Under these conditions VCR resistance decreased from 100-fold to 10-fold. The reversing activity of 7.0 μg/200 μl of the ribozyme was essentially identical to that of 3.5 μg/200 μl of the ribozyme. Therefore, we used complexes made from 0.7 μg/200 μl of DOTAP and 3.5 μg/200 μl of the ribozyme in subsequent experiments. The identical procedure failed to reverse MDR in MOLT-3/TMQ_{800} cells (data not shown).

Next, we examined the specificity of MDR reversal by using various controls. In this experiment both parent MCF-7 and MCF-7/R cells were treated with the DOTAP-*MDR*1 ribozyme complex for 5 consecutive days. Controls included DOTAP on day 0 only or for 5 consecutive days, ribozyme only for 5 consecutive days and

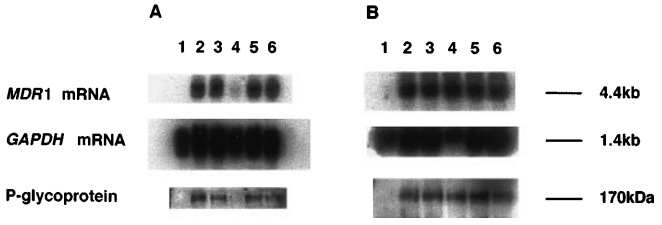

Fig. 4A,B For Northern blot analysis total cellular RNA was extracted by the acid guanidinium thiocyanate-phenol-chloroform method. Total RNA (5 μg per lane) was applied to 1% agarose gel containing formaldehyde; electrophoresis was then performed. After electrophoresis, RNA was transferred to a BA-SNC nitrocellulose membrane (Schleicher & Schuell, Keene, N.H.) and hybridized with probes labeled with α[^{32}P]-dCTP (Du Pont, Boston, Mass.). The cDNA for *MDR*1 (pMDR 2000XS, kindly provided by Dr. M. Gottesman of the National Cancer Institute, Bethesda, Md.) and the cDNA for GAPDH (Clontech, Palo Alto, Calif.) were used as probes. For Western blot analysis protein was solubilized and extracted using a standard protocol. Protein (10 μg per lane) was separated by electrophoresis on 6% SDS-polyacrylamide gel, transferred to BA-SNC nitrocellulose membrane and probed with P-glycoprotein-specific monoclonal antibody C494 (Signet, Dedham, Mas.). The membrane was exposed to [^{125}I]-protein A (Amersham, Arlington Heights Ill.) and autoradiography was performed. **A** *MDR*1 expression by MCF-7/R cells in the presence of DOTAP-*MDR*1 ribozyme complex (*lane 1* MCF-7 cells, *lane 2* MCF-7/R cells, *lane 3* MCF-7/R cells treated with DOTAP alone for 5 days, *lane 4* MCF-7/R cells treated with the complex for 5 days, *lane 5* MCF-7/R cells treated with DOTAP alone for 1 day only (day 0), *lane 6* MCF-7/R cells treated with the complex for 1 day only). *MDR*1 expression and P-glycoprotein production by MCF-7/R cells were almost completely downregulated when cells were incubated with the complex for 5 days. **B** *MDR*1 expression by MOLT-3/TMQ_{800} cells in the presence of the complex (*lane 1* MOLT-3 cells, *lane 2* MOLT-3/TMQ_{800} cells, *lane 3* MOLT-3/TMQ_{800} cells treated with DOTAP alone for 5 days, *lane 4* MOLT-3/TMQ_{800} cells treated with the complex for 5 days, *lane 5* MOLT-3/TMQ_{800} cells treated with DOTAP alone for 1 day only (day 0), *lane 6* MOLT-3/TMQ_{800} cells treated with the complex for 1 day only)

the DOTAP-ribozyme complex on day 0 only. The results are shown in Fig. 3. As expected, the treatment with the complex for 5 consecutive days resulted in the reversal of VCR sensitivity in MCF-7/R cells, whereas none of the control treatments affected the dose-effect curve. Treatment for 5 days with the complex did not affect the dose-effect curve of the parent MCF-7 cells. As for MOLT-3/TMQ_{800} cells, none of the treatments affected VCR sensitivity.

In an attempt to explain the differential sensitivity of the two cell lines against the liposome-ribozyme treatment, *MDR*1 expression was determined and the results are shown in Fig. 4. When MCF-7/R cells were incubated with the DOTAP-ribozyme complex for 5 consecutive days *MDR*1 mRNA expression was almost completely downregulated and P-glycoprotein was barely detectable. When cells were treated with DOTAP-ribozyme complex for 1 day only or DOTAP only for 5 days, *MDR*1 mRNA expression and the amount of P-glycoprotein were unaffected. MOLT-3/TMQ_{800} cells showed equal *MDR*1 mRNA expression and amount of P-glycoprotein under all experimental conditions examined.

In a further attempt to explain the differential effects, the endocytotic activities of the two cell lines were determined. Figure 5 illustrates the results of the phase-contrast microscopic study. When exposed to DOTAP, MCF-7/R cells became rounded and many cyclic homogeneous cytoplasmic vacuoles developed (Fig. 5C). When exposed to latex beads, MCF-7/R cells developed a shiny material in the cytoplasm of all cells, possibly as a result of reflection from the latex beads (Fig. 5E). In contrast, when exposed to DOTAP, MOLT-3/TMQ_{800} cells developed hardly any cytoplasmic vacuoles. The diameter and shape of these cells were nearly the same as control cells (Fig. 5D). Similarly, when MOLT-3/TMQ_{800} cells were exposed to latex beads, although some cells became larger, the shiny material was not seen (Fig. 5F).

The uptake of DOTAP or latex beads into MCF-7/R cells was confirmed by confocal microscopic imaging (Fig. 6). In the presence of DOTAP-FITC-dextran complex (Fig. 6C) or FITC-conjugated latex beads (Fig. 6E) definite fluorescence was seen in the cytoplasm of MCF-7/R cells. In contrast, hardly any fluorescence was seen in either MCF-7/R cells in the medium only (data not shown) or in the presence of FITC-dextran only (Fig. 6A). In MOLT-3/TMQ_{800} cells fluorescence was hardly detected under any of the experimental conditions. To ensure that uptake by MCF-7/R cells was a result of endocytosis, the effects of cytochalasin B pretreatment on the uptake of DOTAP-FITC-dextran

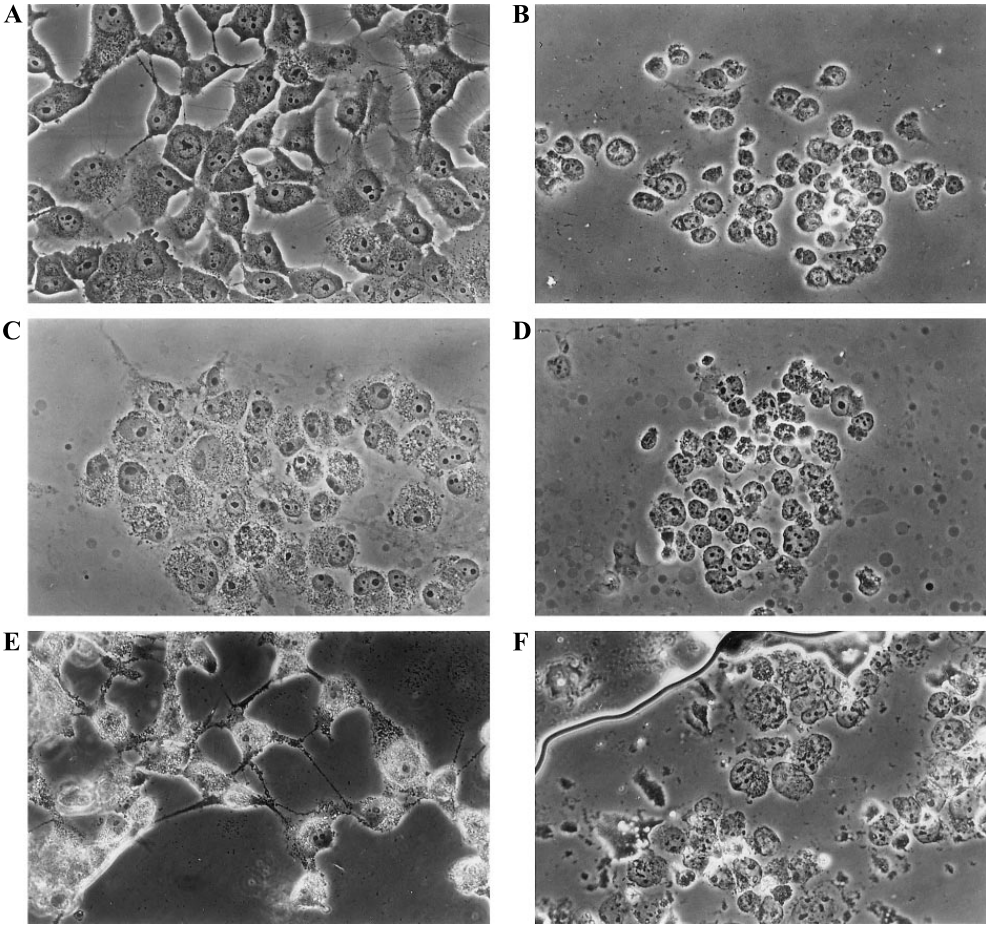

Fig. 5A–F Phase-contrast microscopy of MCF-7/R and MOLT-3/TMQ_{800} cells.MCF-7/R cells (**A**, **C**, **E**) or MOLT-3/TMQ_{800} cells (**B**, **D**, **F**) were incubated for 48 h with medium only as control (**A**, **B**), with 0.35% DOTAP (**C**, **D**) or with latex beads (**E**, **F**) (×200)

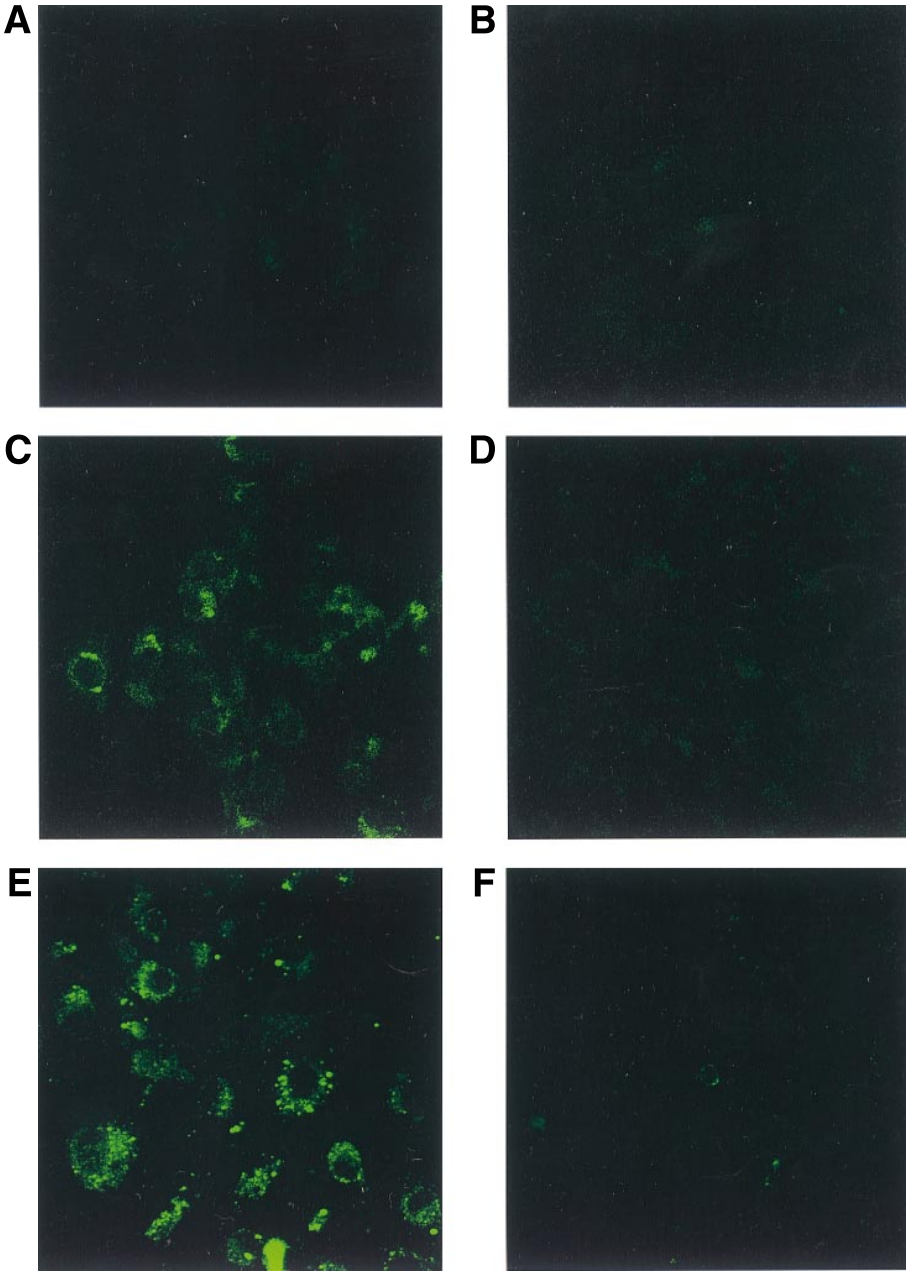

Fig. 6A–F Confocal microscopy (×250). MCF-7/R (**A**, **C**, **E**) or MOLT-3/TMQ_{800} cells (**B**, **D**, **F**) were grown in the presence of FITC-dextran only (**A**, **B**), DOTAP-FITC-dextran complex (**C**, **D**) or FITC-conjugated latex beads (**E**, **F**). FITC fluorescence was detected by confocal imaging using a Leica True Confocal Scanner 4D system (Leica, Deerfield, Ill.) equipped with an argon krypton laser coupled to a Leica Leitz DMR fluorescence microscope and a 40× Plan Fluotar oil objective. Successive images, were rendered using Adobe Photoshop 3.0 software (Adobe Systems, Mountain View, Calif.)

complex or FITC-conjugate latex beads were examined by confocal microscopy (Fig. 7). Cytochalasin B is known to inhibit endocytosis [17, 18]. Definite fluorescence was seen in MCF-7/R cells not treated with cytochalasin B (Fig. 7A,C), whereas little fluorescence was seen in cells pretreated with cytochalasin (Fig. 7B, D). Trypan blue dye exclusion showed the MCF-7/R and MOLT-3/TMQ_{800} cells to be more than 95% viable under these experimental conditions.

These results indicate that MCF-7/R cells can take up the DOTAP-FITC-dextran complex or FITC-conjugate latex beads, whereas with MOLT-3/TMQ_{800} cells there was hardly any uptake. MCF-7/R cells have definite endocytotic activity, whereas MOLT-3/TMQ_{800} cells have little.

Discussion

In the study reported here we examined the effectiveness of the ribozyme transferred by cationic liposome into two P-glycoprotein-positive human tumor cell lines exhibiting the MDR phenotype, MCF-7/R and MOLT-3/TMQ_{800}. We observed that liposome-mediated transfer of *MDR*1 ribozyme RNA produced reversal of the MDR phenotype only in certain cells. In order for this approach to be effective, (a) the liposome-RNA complex must be present for a certain period of time, and (b) target cells must have endocytotic activity.

We noted that the DOTAP-*MDR*1 ribozyme complex seemed less toxic than DOTAP only (Tables 1

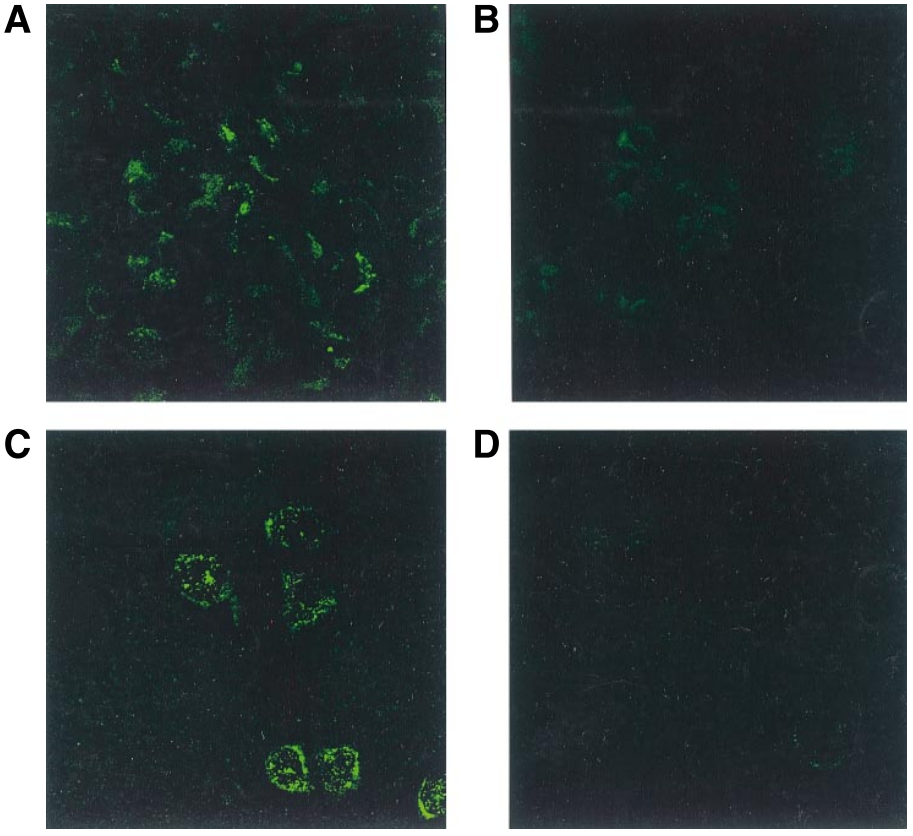

Fig. 7A–D Effects of cytochalasin B on the uptake of DOTAP-FITC-dextran complex or FITC-conjugated latex beads (×250). MCF-7/R cells incubated with DOTAP-FITC-dextran complex (**A**, **B**) or FITC-conjugated latex beads (**C**, **D**) after pretreatment with cytochalasin B (**B**, **D**) or without pretreatment (**A**, **C**) were examined by confocal microscopy

and 2). The presence of the ribozyme might have reduced the cytotoxic effects of DOTAP. It has been reported that the cytotoxicity of cationic liposome correlates well with the amount of its positive charge [19]. Since ribozyme has a negative charge, it can neutralize the positive charge of DOTAP to some extent when the complex is formed. This could explain why the DOTAP-ribozyme complex was less cytotoxic than DOTAP itself. It has also been reported that cationic liposome-ribozyme complexes attach to the cell membrane of target cells via attraction between their positive charge and the negative charge of the cell membrane [16]. This means that transfer efficiency might be reduced if excess ribozyme were present. This could explain the finding that reversal of MDR with the complex containing 7.0 μg/200 μl of the ribozyme was not more efficacious than that with 3.5 μg/200 μl of the ribozyme.

MCF-7/R cells incubated with the daily addition of the DOTAP-*MDR*1 ribozyme complex became more VCR-sensitive with a decrease in *MDR*1 expression, whereas MCF-7/R cells to which the DOTAP-*MDR*1 ribozyme complex was added on day 0 only did not show reversal of VCR resistance. These findings indicate that the approach was effective only if cells were continuously exposed to the complex for certain periods of time. It is possible that some decrease in *MDR*1 expression might have occurred on day 1 in samples to which the complex was added on day 0 only. If this were the case, the amounts of *MDR*1 mRNA and P-glycoprotein had returned to the level of untreated cells by day 5. Our findings are consistent with those reported by Kiehntopf et al. [20], in which liposome-ribozyme complex was added every 12 h over a total period of 72 h. We did not measure either the half-life of the ribozyme within the cell or endogenous nuclease activities. Such information may be useful to explain the lack of biological effects from 1 day of exposure and to develop an exposure schedule on a rational basis. The minimum effective exposure time is yet to be determined.

Treatment of MCF-7/R cells with the complex for 5 days resulted in almost complete downregulation of *MDR*1 mRNA and nearly complete abolition of P-glycoprotein production (Fig. 4). In spite of this, we found that a tenfold higher VCR resistance remained in the treated cells. This may be related to the fact that the MCF-7/R cells were naturally selected to DXR and that multiple mechanisms of MDR may exist in these cells.

In attempts to explain the differential effects of the liposome-*MDR*1 ribozyme complex against the two P-glycoprotein-producing cell lines we evaluated by phase-contrast and confocal microscopy the uptake of DOTAP and latex beads. Lipids can form cationic liposomes 250 nm in diameter [16]. The latex beads used were of a similar size, about 240 nm in diameter. When MCF-7/R cells were incubated with DOTAP, cytoplasmic vacuoles developed (Fig. 5C). Bonnekoh et al. [21] have reported that human keratinocytes show cyclic and polycyclic homogeneous vacuoles by phase-contrast microscopy when they take up liposomes with no direct cytotoxic effect. As the morphological changes observed

in our experiments were identical to theirs, it is likely that liposomes were incorporated within the cells. When MCF-7/R cells were incubated with latex beads, shiny material was observed in the cytoplasm (Fig. 5E). This finding is consistent with that reported by Veras et al. [22] who showed that latex beads taken up by Chinese hamster ovary cells shine under a phase-contrast microscope. This suggests light reflection from the latex beads. In contrast, in MOLT-3/TMQ_{800} cells hardly any morphological changes were observed in the presence of DOTAP or latex beads and there was no evidence that DOTAP or latex beads had entered the cells.

In the experiments with confocal microscopy, because the molecular weight of *MDR*1 ribozyme used here was about 12 000 Da, FITC-dextran of molecular weight about 10 000 Da was used. Definite fluorescence was observed in the cytoplasm when MCF-7/R cells were incubated with DOTAP-FITC-dextran complex or FITC-conjugated latex beads, whereas fluorescence was hardly observed in MOLT-3/TMQ_{800} cells under any experimental conditions. The experiments with cytochalasin B further reinforced our hypothesis that the uptake by MCF-7/R cells was a result of endocytosis. The success of liposome-mediated delivery may thus be predicted by determination of the endocytotic activity of the target tumor cells.

Acknowledgements The authors acknowledge support by the T.J. Martell Memorial Foundation for Leukemia, Cancer and AIDS Research, New York, by the United Leukemia Fund, New York, and by the Chemotherapy Foundation, New York.

References

1. Ling V (1985) Multidrug resistant mutants. In: Gottesman MM (ed) Molecular cell genetics. John Wiley, New York, p 773
2. Pastan I, Gottesman MM (1987) Multiple-drug resistance in human cancer. N Engl J Med 316: 1388
3. Croop JM, Gros P, Housman DE (1988) Genetics of multidrug resistance. J Clin Invest 81: 1303
4. Endicott JA, Ling V (1989) The biochemistry of P-glycoprotein-mediated multidrug resistance. Annu Rev Biochem 58: 137
5. Fuqua SAW, Morreti-Rojas IM, Schneider SL, McGuire WL (1987) P-glycoprotein expression in human breast cancer cells. Cancer Res 47: 2103
6. Lemontt JF, Azzaria M, Gros P (1988) Increased mdr gene expression and decreased drug accumulation in multidrug-resistant human melanoma cells. Cancer Res 48: 6348
7. Li X-K, Kobayashi H, Holland JF, Ohnuma T (1993) Expression of dihydrofolate reductase and multidrug resistance genes in trimetrexate-resistant human leukemia cell lines. Leuk Res 17: 483
8. Cech TR (1988) Ribozymes and their medical implications. JAMA 260: 3030
9. Haseloff J, Gerlach WJ (1988) Simple RNA enzymes with new and highly specific endoribonuclease activities. Nature 334: 585
10. Marschall P, Thomson JB, Eckstein F (1994) Inhibition of gene expression with ribozymes. Cell Mol Neurobiol 14: 523
11. Kobayashi H, Dorai T, Holland JF, Ohnuma T (1994) Reversal of drug sensitivity in multidrug-resistant tumor cells by an MDR1 (PGY1) ribozyme. Cancer Res 54: 1271
12. Holm PS, Scanlon KJ, Dietel M (1994) Reversion of multidrug resistance in the P-glycoprotein-positive human pancreatic cell line (9EPP85-181RDB) by introduction of a hammerhead ribozyme. Br J Cancer 70: 239
13. Cowan KH, Batist G, Tulpule A, Sinha B, Myers CE (1986) Similar biochemical changes associated with multidrug resistance in human breast cancer cells and carcinogen-induced resistance to xenobiotics in rats. Proc Natl Acad Sci USA 83: 9328
14. Minowada J, Ohnuma T, Moore GE (1972) Rosette-forming human lymphoid cell lines: 1. Establishment and evidence for origin of thymus-derived lymphocytes. J Natl Cancer Inst 49: 891
15. Milligan JF, Groebe DR, Witherell GW, Uhlenbeck OC (1987) Oligoribonucleotide synthesis using T7 RNA polymerase and synthetic DNA templates. Nucl Acids Res 15: 8783
16. Felgner PL, Ringold GM (1989) Cationic liposome-mediated transfection. Nature 337: 387
17. Takigawa N, Danno K, Furukawa F (1987) Effects of colchicine and cytochalasin B on distribution of concanavalin A receptors in isolated and cultured guinea pig epidermal cells. Arch Dermatol Res 279: 392
18. Finbloom DS, Martin J, Gordon RK (1987) Endocytosis of particulate and soluble IgG immune complexes: differential effects of cytoskeletal modulating agents. Clin Exp Immunol 67: 205
19. Huang L, Farhood H, Serbina N, Teepe AG, Barsoum J (1995) Endosomolytic activity of cationic liposomes enhances the delivery of human immunodeficiency virus-1 transactivator protein (TAT) to mammalian cells. Biochem Biophys Res Commun 217: 761
20. Kiehntopf M, Brach MA, Licht T, Petschauer S, Karawajew L, Kirschning C, Herrmann F (1994) Ribozyme-mediated cleavage of the MDR1 transcript restores chemosensitivity in previously resistant cancer cells. EMBO J 13: 4645
21. Bonnekoh B, Roeding J, Krueger GRF, Ghyczy M, Mahrle G (1991) Increase of lipid fluidity and suppression of proliferation resulting from liposome uptake by human keratinocytes in vitro. Br J Dermatol 124: 333
22. Veras PST, de Chastellier C, Moreau M-F, Villers V, Thibon M, Mattei D, Rabinovitch M (1994) Fusion between large phagocytic vesicles: targeting of yeast and other particulates to phagolysosomes that shelter the bacterium *Coxiella burnetii* or the protozoan *Leishmania amazonesis* in Chinese hamster ovary cells. J Cell Sci 107: 3065